Research Article

Asymmetric Photoaerobic Lactonization and Aza-Wacker Cyclization of Alkenes Enabled by Ternary Selenium−Sulfur Multicatalysis

Tao Lei,[†] Sebastian Graf,[†] Christopher Schöll, Felix Krätzschmar, Bernhard Gregori, Theresa Appleson, and Alexander Breder*

Cite This: *ACS Catal.* 2023, 13, 16240−16248

Read Online

ACCESS | 📊 Metrics & More | 📰 Article Recommendations | 🆂🅸 Supporting Information

ABSTRACT: An adaptable, sulfur-accelerated photoaerobic selenium-π-acid ternary catalyst system for the enantioselective allylic redox functionalization of simple, nondirecting alkenes is reported. In contrast to related photoredox catalytic methods, which largely depend on olefinic substrates with heteroatomic directing groups to unfold high degrees of stereoinduction, the current protocol relies on chiral, spirocyclic selenium-π-acids that covalently bind to the alkene moiety. The performance of this ternary catalytic method is demonstrated in the asymmetric, photoaerobic lactonization and cycloamination of enoic acids and unsaturated sulfonamides, respectively, leading to an averaged enantiomeric ratio (er) of 92:8. Notably, this protocol provides for the first time an asymmetric, catalytic entryway to pharmaceutically relevant 3-pyrroline motifs, which was used as a platform to access a 3,4-dihydroxyproline derivative in only seven steps with a 92:8 er.

method features:
- 1st asymm. catalytic 3-pyrroline synthesis
- *er* up to 97:3
- modular Se-catalyst architecture

KEYWORDS: enantioselectivity, photoredox catalysis, chiral selenium-π-acids, alkenolides, 3-pyrrolines, 1,1'-spirobiindane
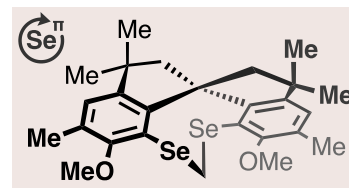
■ INTRODUCTION

The design of highly enantioselective catalytic procedures for the economic manufacture of chiral molecules represents an integral and swiftly proliferating area within modern chemical synthesis.[1] Throughout the last decades, a rapidly increasing number of efforts toward the development and customization of chiral catalyst motifs has led to stereochemically well-controlled transformations in many relevant reaction categories. A striking exception to this state of affairs in chemical methodology are enantioselective photoredox-catalytic functionalizations of simple, nondirecting alkenes. Looking at asymmetric photoredox catalysis in its current state,[2] most protocols predicate on the covalent or noncovalent binding of the photocatalyst or a cocatalyst to a heteroatomic binding site within the substrate. Most prominent examples include—but are not limited to—carbonyls,[3] heteroarenes,[4] β-ketoesters,[5] amides,[6] imines,[7] and carboxylic esters[8] (Scheme 1). Elegant early contributions to this field were made, inter alia, by Bach and co-workers who reported on the asymmetric intra-molecular conjugate addition of pyrrolidin-2-yl radicals onto Michael acceptors.[6a] Stereocontrol was accomplished by means of a H-bonding catalyst derived from Kemp's acid (Scheme 1a). Subsequently, other radical conjugate addition reactions governed by complementary stereocontrolling principles such as asymmetric iminium/enamine catalysis (Scheme 1b),[9] Lewis/Brønsted-acid catalysis (Scheme 1c),[10] and enzyme catalysis[11] were put on record. Two early and very instructive

examples, emphasizing the decisive impact of the nature of substrate−catalyst interactions in enantioselective photoredox catalysis, were described by Ooi et al. and Nicewicz et al. in their reports on asymmetric [3 + 2] and [4 + 2]-cycloadditions, respectively (Scheme 1g,h).[12,13] Each method predicated on a chiral counteranion as the stereocontrolling element. In the former case, a photoredox-active iridium(III) complex, harboring a chiral borate anion, was used as a catalyst.[12] The anion was able to sustain an H-bond interaction with one of the reactants (Scheme 1g), which was crucial for the high enantiomeric ratio (er) of up to 98.5:1.5. In the second case, the authors employed a triphenylpyrylium catalyst possessing a chiral phosphoric amide counterion, which interacted with transient radical cationic intermediates dominantly through electrostatic forces (Scheme 1d,h) and furnished the cycloadducts in er values of ≤75:25.[13,14] These results emphasize the challenges caused by alkenes lacking any heteroatomic binding sites for a catalyst. Two rare yet very noteworthy tactics to address even nondirected alkenes were recently reported. On the one hand, certain copper catalysts
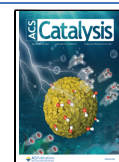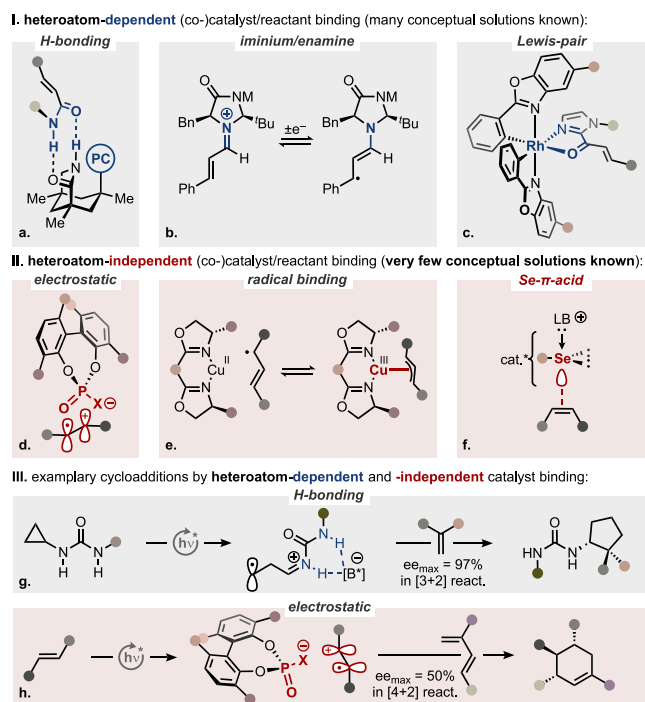
Scheme 1. Heteroatom-Dependent and -Independent Binding Concepts in Asymmetric Photoredox Catalysis[a]

[a](I) Simplified representations of heteroatom-dependent catalyst/reactant binding modes in enantioselective photoredox-catalytic alkene functionalizations. (II) Simplified representations of heteroatom-independent catalyst/reactant binding modes. (III) Exemplary comparison of counterion binding modes in asymmetric photoredox-catalysis ([B*]⁻ = chiral borate anion, X = O or NTf).

were used in asymmetric ATRA reactions, in which Cu covalently binds to a carbon-centered radical intermediate, which derived from the alkene (Scheme 1e).[15a−bcd] On the other hand, List et al. reported on the asymmetric counterion-directed photoredox catalytic [2 + 2] cycloaddition of alkenes, in which sterically confined imidophosphorimidates served as highly efficient stereoinducing cocatalysts.[15e] Each of these protocols is very substrate-specific, insofar as they are compatible with only terminal and/or conjugated olefins. Consequently, more structure-tolerant solutions for asymmetric, photoredox-catalytic functionalizations of nondirected, internal alkenes remain elusive.

Recently, selenium-π-acids[16] were introduced as efficient main group complements to redox-active transition metals in photoredox-catalytic alkene functionalizations.[16,17] Mechanistically, Se-π-acids proved effective for certain alkene motifs (e.g., acyclic, nonconjugated, 1,2-dialkylated [alkyl > Me]) that were not tolerated by previous catalytic protocols.[17] More concretely, photoaerobic selenium-π-acid multicatalysis operates by a radical−polar crossover mechanism,[16a,acde,−,18,18] which allows for an overall ionic, two-electron oxidation of alkenes under single-electron-transfer conditions. This circumstance entails the advantage that O_2 (or even air) can be used as a terminal oxidant[19] since O_2-sensitive, carbon-centered radicals or radical ions, which normally epitomize customary photoredox-catalysis, are not formed under operating conditions. Furthermore, selenium-π-acids interact with their olefinic substrates through dynamic covalent binding to the carbon−carbon π-bond (Scheme 1f), which opens the
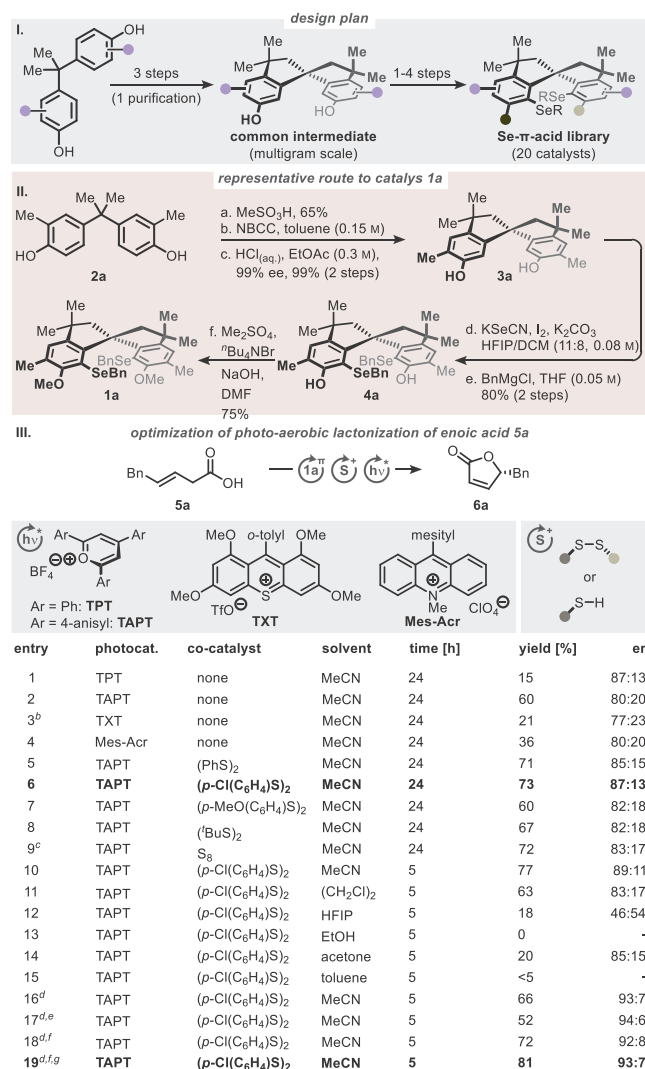
opportunity to induce stereochemical information by means of chiral selenium species under photocatalytic conditions. However, previous efforts in this direction only met with limited success, leading to average er values distinctly below 75:25.[20,21] As a viable solution to previously encountered difficulties, we now report the design of a modular, spirocyclic selenium-π-acid motif, which allows for the photocatalytic, enantioselective lactonization and amination of nondirecting, internal alkenes under the assistance of sulfur cocatalysts to provide access to various chiral alkenolides and—*for the first time*—3-pyrrolines.

RESULTS AND DISCUSSION

From preliminary work on photoaerobic lactonizations, we realized that the degree of stereoinduction of a given chiral selenium-π-acid roughly correlated with its conformational rigidity.[20] This notion is in good agreement with very insightful reports by Maruoka et al., Denmark et al., and others on thermal selenium-π-acid-catalyzed alkene functionalizations.[22] Hence, we decided to investigate the 1,1′-spirobiindane skeleton[23] as a versatile yet highly rigid platform to design a structurally and electronically adjustable library of selenium-π-acids (Schemes 2 and 3). Our initial efforts focused on two objectives: (a) a divergent synthetic route to target catalyst 1 from common, readily available building blocks (Scheme 2I) and (b) an easily adjustable periphery around the Lewis-acidic selenium centers (Scheme 3).

Synthesis of catalyst 1a commenced with the exposure of bisphenol A (2a) to a 20-fold excess of methanesulfonic acid, which gave the corresponding racemic spirobiindane-6,6′-diol in a 65% yield (Scheme 2II).[24] Resolution of the racemate by cocrystallization with N-benzylcinchonidinium chloride provided (+)-(R)-3a in a 99% yield and 99% ee upon workup.[25] Oxidative selenation of 3a was subsequently accomplished with KSeCN and iodine followed by substitution of the cyanide groups with BnMgCl, furnishing 4a in an 80% yield.[26] Completion of 1a involved the methylation of the 6/6′ hydroxy groups with Me_2SO_4 (75% yield), thus showcasing that the desired catalyst motif 1 can be accessed expediently in a total yield of 39% over six steps. This route was then used as a blueprint for the synthesis of catalysts 1b−t shown in Scheme 3 (for details, see the Supporting Information).[27−29]

Next, we evaluated the catalytic performance of catalysts 1a−t in the photoaerobic asymmetric lactonization of 5-phenyl pent-2-enoic acid (5a, Schemes 2III and 3). Acid 5a was initially exposed to a small series of photoredox catalysts (Scheme 2III, entries 1−4) in combination with Se-π-acid catalyst 1a under air and 465 nm irradiation at 18 °C in MeCN (0.1 M) for 24 h. 2,4,6-Tris(p-anisyl)pyrylium tetrafluoroborate (TAPT) turned out to give the best yield (60%) of (S)-butenolide 6a with an er of 80:20 (entry 2).[30] A screening for sulfur cocatalysts (entries 5−9)[30] revealed that disulfides (5 mol %), thiols (10 mol %), and even elemental sulfur (10 mol % of S_8) significantly accelerated the title process, leading to increased yields of up to 73% (entry 6) and er values of up to 87:13 (entries 2, 5−9). In this context, we noticed that under disulfide cocatalysis, the reaction time can be reduced to 5 h without negative effects on the yield or er values (entry 10, yield = 77%, er = 89:11). Notably, in the absence of sulfur cocatalysts or in the presence of any other non-sulfur additives tested, the lactonization became very sluggish and unproductive with yields less than 36% within 5 h (Scheme S4, Table S1). Initial kinetic rate studies (Figures S1−S4) indicate that

Scheme 2. Catalyst Design Plan and Reaction Optimization[a]

I. *design plan*

3 steps (1 purification) → **common intermediate** (multigram scale) → 1-4 steps → **Se-π-acid library** (20 catalysts)

II. *representative route to catalys 1a*

2a
a. MeSO₃H, 65%
b. NBCC, toluene (0.15 M)
c. HCl(aq.), EtOAc (0.3 M), 99% ee, 99% (2 steps) → **3a**

d. KSeCN, I₂, K₂CO₃ HFIP/DCM (11:8, 0.08 M)
e. BnMgCl, THF (0.05 M) 80% (2 steps) → **4a**

f. Me₂SO₄, ⁿBu₄NBr NaOH, DMF 75% → **1a**

III. *optimization of photo-aerobic lactonization of enoic acid 5a*

5a — (1a)(S)(hv) → **6a**

Ar = Ph: **TPT**
Ar = 4-anisyl: **TAPT**

TXT

mesityl **Mes-Acr**

entry	photocat.	co-catalyst	solvent	time [h]	yield [%]	er
1	TPT	none	MeCN	24	15	87:13
2	TAPT	none	MeCN	24	60	80:20
3[b]	TXT	none	MeCN	24	21	77:23
4	Mes-Acr	none	MeCN	24	36	80:20
5	TAPT	(PhS)₂	MeCN	24	71	85:15
6	**TAPT**	**(p-Cl(C₆H₄)S)₂**	**MeCN**	**24**	**73**	**87:13**
7	TAPT	(p-MeO(C₆H₄)S)₂	MeCN	24	60	82:18
8	TAPT	(ᵗBuS)₂	MeCN	24	67	82:18
9[c]	TAPT	S₈	MeCN	24	72	83:17
10	TAPT	(p-Cl(C₆H₄)S)₂	MeCN	5	77	89:11
11	TAPT	(p-Cl(C₆H₄)S)₂	(CH₂Cl)₂	5	63	83:17
12	TAPT	(p-Cl(C₆H₄)S)₂	HFIP	5	18	46:54
13	TAPT	(p-Cl(C₆H₄)S)₂	EtOH	5	0	-
14	TAPT	(p-Cl(C₆H₄)S)₂	acetone	5	20	85:15
15	TAPT	(p-Cl(C₆H₄)S)₂	toluene	5	<5	-
16[d]	TAPT	(p-Cl(C₆H₄)S)₂	MeCN	5	66	93:7
17[d,e]	TAPT	(p-Cl(C₆H₄)S)₂	MeCN	5	52	94:6
18[d,f]	TAPT	(p-Cl(C₆H₄)S)₂	MeCN	5	72	92:8
19[d,f,g]	**TAPT**	**(p-Cl(C₆H₄)S)₂**	**MeCN**	**5**	**81**	**93:7**

[a](I) General approach toward chiral selenium-π-acid catalysts. (II) Exemplary synthetic route toward catalyst **1a**. NBCC = N-benzyl cinchonidinium chloride; HFIP = 1,1,1,3,3,3-hexafluoropropan-2-ol. (III) Reaction condition: n₍₅ₐ₎ = 0.3 mmol, c₍₅ₐ₎ = 0.1 M, photocat. (entries 1–9: 5 mol %; entries 10–19: 10 mol %), **1a** (10 mol %), cocatalyst (5 mol %), 18 °C, air, irradiation at 465 nm, isolated yield. [b]Irradiation at 528 nm. [c]10 mol % of S₈. [d](SiMe₃)₂ (1.0 equiv) was added. [e]Catalyst **1d** (10 mol %, Scheme 3) was used. [f]Catalyst **1i** (10 mol %, Scheme 3) was used. [g]0.5 mmol of **5a** [c₍₅ₐ₎ = 0.1 M] was used. TPT = 2,4,6-triphenylpyrylium tetrafluoroborate; TAPT = 2,4,6-tris(p-anisyl)pyrylium tetrafluoroborate; TXT = 1,3,6,8-tetramethoxy-9-(o-tolyl)thioxanthylium trifluoromethanesulfonate.
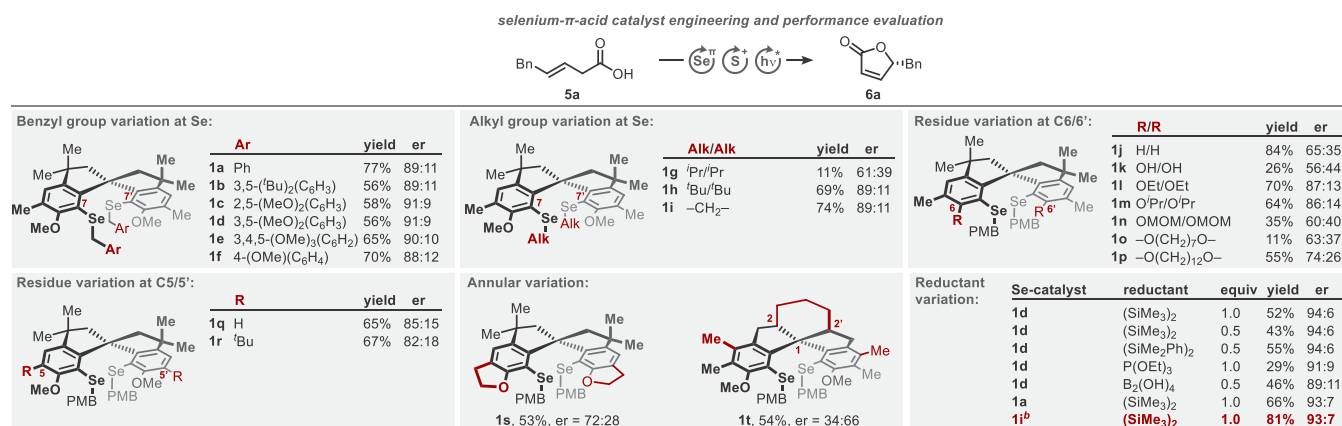
substoichiometric amounts of disulfide not only reduce the initiation phase required for the conversion of the bis-selane catalyst **1a** into its active form but also increase the turnover rate upon full liberation of the active selenium species.[31] In addition, we could confirm that no product formation was observed when the Se catalysts or the photoredox catalysts were omitted from the title reaction, as was the case when the lactonization was attempted in the dark (Table S1).

At this stage, the impact of structural modifications on catalysts **1b–t** was evaluated. Electronic variation of the benzylic Se-protecting groups (i.e., 7/7′ position, Scheme 3)

showed no particular trend with regard to the er values, which remained between 88:12 and 91:9 (Scheme 3, **1a–f**). Changing the protection group to an aliphatic protecting group had a more significant influence. More specifically, the *tert*-butyl (**1h**) and methylene (**1i**) groups resulted in markedly higher yields relative to the more stable *iso*-propyl residue (**1g**). We suspect that the yield and stereoselectivity correlate with the facility by which the Se-protecting groups can be removed under the title conditions. More concretely, the more stabilized the suspected cationic fragments from the former Se-protecting groups are[32] (i.e., selenocarbenium ion from **1i** vs 2-methylpropan-2-ylium ion from **1h** vs propan-2-ylium ion from **1g**), the more easily they furnish access to the active Se catalyst. Overall, these results show that more fissile protecting groups weakly correlate with increasing yields but do not affect the stereoinduction.
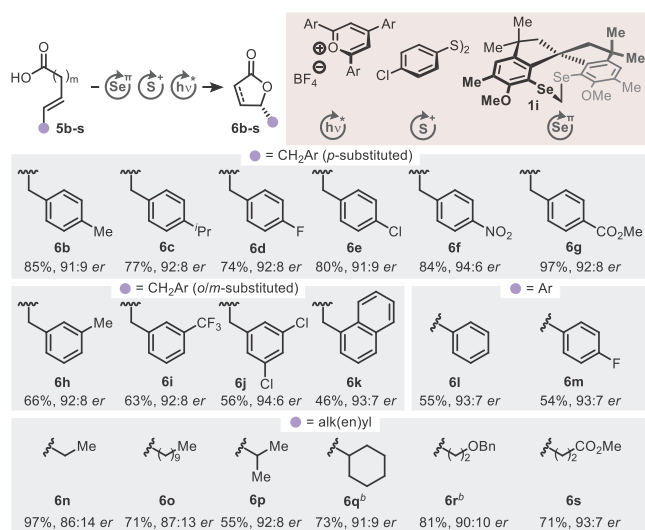
Continuing with modifications at position 6/6′ revealed that the oxygen atoms seem to play a significant role for the stereoinduction. While the removal of the OMe group or its replacement for an OH group (**1j/k**) had detrimental effects on the er, other simple alkyl ether groups (**1l/m**) showed performances similar to that of **1a**. This observation is in line with reports by Wirth and Tomoda et al., who demonstrated that n → σ* O···Se nonbonding interactions typically result in rigidified catalyst–substrate conformations and thus in higher levels of stereoinduction.[33] Changing to methoxymethyl groups (**1n**) or bridging ether residues (**1o/p**) provided poorer results, probably due to interference of these residues with the alkene substrate. As anticipated, modification at the distal 5/5′ position (**1q/r**) had no meaningful influence on the reaction outcome. But in contrast to our intuition, further rigidifying the catalyst skeleton through additional annulations (**1s/t**) led to poorer stereoinduction. For **1s**, we interpret this outcome as a result of conformational restrictions at the 6/6′ O atoms, which potentially obviate efficient n → σ* O···Se overlap. Regarding catalyst **1t**, bite angles (i.e., relative orientation of the indane planes at the C1 junction point) of about 87–90° were reported for closely related 2,2′-annelated spirobiindanes.[24b,34] Considering that catalyst **1a** possesses a significantly narrower bite angle of only 73.19° (Figure S5), this difference may be an explanation for the diminished stereoinduction of **1t**.

An important observation was made with catalyst **1a**, which furnished butenolide **6a** after 5 h with an er of 91:9 and 33% yield in the absence of a sulfur cocatalyst (Scheme S4). When the same reaction was conducted for 24 h (Scheme 2, entry 2), the er had dropped to 80:20. We speculate that this outcome results from partial Se oxidation,[35] giving access to oxygenated selenium species that still retain some catalytic activity with lower or opposite enantioselection. To test this hypothesis and suppress the suspected Se oxygenation, we resorted to a recent report by Iaroshenko et al. on the deoxygenative activity of silanes and disilanes on N- and P-oxygenated compounds.[36] To our delight, the combination of 1 equiv of hexamethyldisilane with 10 mol % of catalyst **1a** furnished butenolide **6a** in a 66% yield and an er of 93:7 (Schemes S6 and S7). Under these modified conditions, catalysts **1d** and **1i** provided similar er values (94:6 and 93:7, respectively), but catalyst **1i** gave the best yield under fully optimized conditions (Scheme 2, entry 19) and was therefore chosen for further investigations. It should be mentioned that other chiral selenium catalysts reported for thermal asymmetric lactonizations[22b] gave lower er values under photocatalytic conditions (Scheme S7).[20]

Scheme 3. Performance Evaluation of Catalyst Library and Additives[a]

selenium-π-acid catalyst engineering and performance evaluation

Benzyl group variation at Se:

	Ar	yield	er
1a	Ph	77%	89:11
1b	3,5-(^{t}Bu)$_2$(C$_6$H$_3$)	56%	89:11
1c	2,5-(MeO)$_2$(C$_6$H$_3$)	58%	91:9
1d	3,5-(MeO)$_2$(C$_6$H$_3$)	56%	91:9
1e	3,4,5-(OMe)$_3$(C$_6$H$_2$)	65%	90:10
1f	4-(OMe)(C$_6$H$_4$)	70%	88:12

Alkyl group variation at Se:

	Alk/Alk	yield	er
1g	^{i}Pr/^{i}Pr	11%	61:39
1h	^{t}Bu/^{t}Bu	69%	89:11
1i	—CH$_2$—	74%	89:11

Residue variation at C6/6':

	R/R	yield	er
1j	H/H	84%	65:35
1k	OH/OH	26%	56:44
1l	OEt/OEt	70%	87:13
1m	O^{i}Pr/O^{i}Pr	64%	86:14
1n	OMOM/OMOM	35%	60:40
1o	—O(CH$_2$)$_7$O—	11%	63:37
1p	—O(CH$_2$)$_{12}$O—	55%	74:26

Residue variation at C5/5':

	R	yield	er
1q	H	65%	85:15
1r	^{t}Bu	67%	82:18

Annular variation:

1s, 53%, er = 72:28

1t, 54%, er = 34:66

Reductant variation:

Se-catalyst	reductant	equiv	yield	er
1d	(SiMe$_3$)$_2$	1.0	52%	94:6
1d	(SiMe$_3$)$_2$	0.5	43%	94:6
1d	(SiMe$_2$Ph)$_2$	0.5	55%	94:6
1d	P(OEt)$_3$	1.0	29%	91:9
1d	B$_2$(OH)$_4$	0.5	46%	89:11
1a	(SiMe$_3$)$_2$	1.0	66%	93:7
1i[b]	**(SiMe$_3$)$_2$**	**1.0**	**81%**	**93:7**

[a]Reaction conditions: $n_{(5a)}$ = 0.3 mmol, photocat. = 10 mol %, sulfur cat. = 5 mol %, $c_{(5a)}$ = 0.1 M, Temp. = 18 °C, ambient air, 465 nm LED lamps; yields refer to isolated compounds. [b]$n_{(5a)}$ = 0.5 mmol.

After having identified proper catalytic conditions, we analyzed the scope of the title method using structurally and electronically diversified alkenoic acids **5** as substrates (Scheme 4). Initially, a representative series of benzyl analogues of **5a**
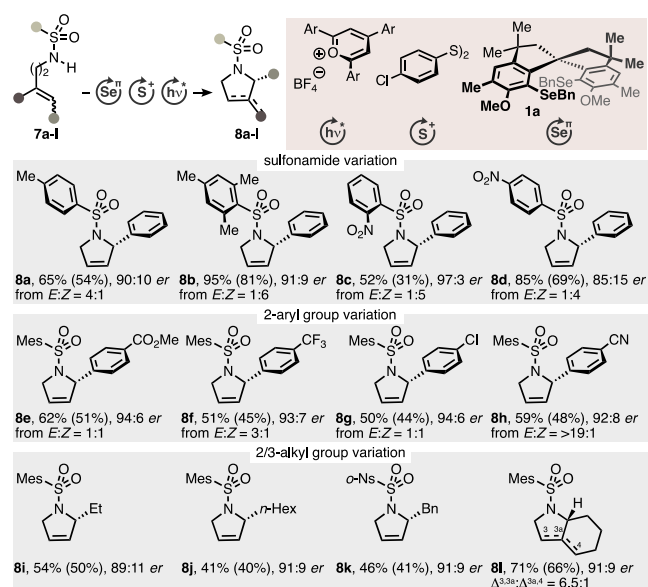
Scheme 4. Substrate Scope of Enantioselective Photoredox-Catalytic Lactonization[a]

• = CH$_2$Ar (*p*-substituted)

6b	**6c**	**6d**	**6e**	**6f**	**6g**
85%, 91:9 er	77%, 92:8 er	74%, 92:8 er	80%, 91:9 er	84%, 94:6 er	97%, 92:8 er

• = CH$_2$Ar (*o*/*m*-substituted) | | | • = Ar

6h	**6i**	**6j**	**6k**	**6l**	**6m**
66%, 92:8 er	63%, 92:8 er	56%, 94:6 er	46%, 93:7 er	55%, 93:7 er	54%, 93:7 er

• = alk(en)yl

6n	**6o**	**6p**	**6q**[b]	**6r**[b]	**6s**
97%, 86:14 er	71%, 87:13 er	55%, 92:8 er	73%, 91:9 er	81%, 90:10 er	71%, 93:7 er

[a]Reaction conditions: $n_{(5b−s)}$ = 0.5 mmol, photocat. = 10 mol % (Ar = 4-methoxyphenyl), **1i** = 10 mol %, sulfur cat. = 5 mol %, $c_{(5b−s)}$ = 0.1 M (MeCN), (SiMe$_3$)$_2$ = 100 mol %, Temp. = 18 °C, ambient air, 465 nm LED lamps. All substrates are *E*-configured. Yields refer to isolated compounds. [b]Reaction was performed with 10 mol % of selenium catalyst **1d**.

was tested. In general, both electron-rich and electron-deficient alkenoic acids **5b−k** provided high er values in the range of 91:9 to 94:6 (Scheme 4). These results already emphasize that our aerobic enantioselective photoredox catalytic protocol is not only distinctly carbon efficient[37] (i.e., use of air instead of carbonous oxidants) but also offers promising levels of stereoinduction in the cyclofunctionalization of alkenes.[17d,20,22,38] In terms of yield, substrates possessing functional groups in the 4-position of the arene ring commonly led to good or very good results (74−97%). Sterically more demanding substrates (i.e., **6h−k**) gave somewhat lower yields

(46−66%) but were as stereoselective as the former analogues. In addition to benzylic substituents, the title procedure also provided good to high stereoinduction with aromatic and aliphatic residues. In the case of aromatic derivatives **6l** and **6m**, yields of 55% and 54%, respectively (er = 93:7 each), were obtained, which is suspected to result from steric factors. This conclusion is supported by the observation that product **6p**, which embeds a bulky *iso*-propyl residue, was obtained in a medium yield of 55% (er = 92:8), while unbranched and conformationally less flexible analogues **6n/o** and **6q−s** gave much better yields (71−97%, er = 87:13 to 93:7).[39] In some cases, substrate degradation was observed, which diminished the product yield and resulted in the formation of carbonyl byproducts. We suspect that this outcome is caused by photocatalytically generated singlet oxygen.

To further explore and generalize the utility of our new enantioselective photoredox-catalytic cyclofunctionalization protocol, we focused on the asymmetric synthesis of 2-substituted 3-pyrrolines (Scheme 5). This compound class has been intensively investigated, inter alia, for their salient role in biologically active natural compounds and pharmaceuticals.[40] Throughout the last 25 years, numerous synthetic protocols for the assembly of chiral 3-pyrroline scaffolds have been reported.[41−45] Most prominent tactics include asymmetric intramolecular S$_N$ reactions,[41] concerted and consecutive cycloadditions,[42] hydroaminations,[43] Mizoroki−Heck reactions,[44] and ring-closing metatheses.[45] Surprisingly, despite the overwhelming progress made in this field, there are no catalytic oxidative enantioselective cycloaminations on record to form 2-substituted 3-pyrroline rings directly.[46] Against this background, we posited that our title method is likely to provide a complementary and unprecedented as well as highly redox-economic[47] entryway. As listed in Scheme 5, sulfonamides **7a−l** were exposed to 10 mol % of Se-catalyst **1a**,[48,49] 10 mol % of *p*-chlorophenyldisulfide, and 5 mol % of TAPT in MeCN under 465 nm irradiation and ambient air (for reaction optimization, see Scheme S8). Gratifyingly, all tested substrates resulted in good to high er values ranging from 85:15 to 97:3 and favoring the *S*-configuration within **8a−l**.[50] In terms of structural variation within the sulfonyl moiety (Scheme 5, **8a−d**, Scheme S9), sterically more demanding residues typically resulted in high er values (e.g., **8b**, 95%, er = 91:9; **8c**, 52%, er = 97:3, Table S2), albeit in partially lower yields.

Scheme 5. Substrate Scope of Enantioselective Photoredox-Catalytic Amination Reaction[a]

8a, 65% (54%), 90:10 er from E:Z = 4:1

8b, 95% (81%), 91:9 er from E:Z = 1:6

8c, 52% (31%), 97:3 er from E:Z = 1:5

8d, 85% (69%), 85:15 er from E:Z = 1:4

2-aryl group variation

8e, 62% (51%), 94:6 er from E:Z = 1:1

8f, 51% (45%), 93:7 er from E:Z = 3:1

8g, 50% (44%), 94:6 er from E:Z = 1:1

8h, 59% (48%), 92:8 er from E:Z = >19:1

2/3-alkyl group variation

8i, 54% (50%), 89:11 er

8j, 41% (40%), 91:9 er

8k, 46% (41%), 91:9 er

8l, 71% (66%), 91:9 er $\Delta^{3,3a}:\Delta^{3,4} = 6.5:1$

[a]Reaction conditions: $n_{(7b-c,e-l)} = 0.5$ mmol, $n_{(7d)} = 0.3$ mmol, photocat. = 5 mol % (Ar = 4-methoxyphenyl), **1a** = 10 mol %, sulfur cat. = 10 mol %, $c_{(7a-l)} = 0.1$ M (MeCN), Temp. = r.t., ambient air, 465 nm LED lamps. Substrates are E-configured if not stated otherwise. Yields of isolated products are given in parentheses. Crude yields were determined by ^{1}H NMR spectroscopy using 1,3,5-trimethoxybenzene as an internal standard.

Overall, the mesityl group of substrate **7b** turned out to be the best compromise between yield and selectivity (Scheme S9). Modification of the Ph residue (**8b**) with different functional groups such as p-CO$_2$Me (**8e**), p-CF$_3$ (**8f**), p-Cl (**8g**), and p-CN (**8h**) resulted in good selectivities (er = 92:8 to 94:6). In addition to secondary alkenes **7i–7k**, tertiary alkene **7l** was also tolerated, which gave a 6.5:1 mixture of 3-pyrroline **8l** and its pyrrolidine isomer but otherwise similar results to the former alkenes (i.e., yields from 41 to 71% and er from 89:11 to 91:9). Two observations are noteworthy in this context: (1) only trace amounts of products **8** were obtained when the sulfur cocatalyst was omitted (e.g., **8a**, 65% with S-cat. vs 6% without S-cat.). This finding underscores the importance of the sulfur species in the asymmetric, photoaerobic cyclofunctionalization of alkenes.[31] (2) For substrates **7a–h**, we found that our ternary catalyst system was able to convert E/Z-mixtures with varying ratios (Schemes 5 and S9) into products **8a–h** with good enantioselectivity. To the best of our knowledge, this feature is unique to this photocatalytic protocol, as related methods strictly rely on purely E-configured substrates.[22] Control experiments showed that the stereoconvergence most likely results from rapid Z-to-E-isomerization of the substrates prior to selenium-catalyzed conversion into products **8a–h** (Scheme S9 and Figure S7).

To eventually showcase the practicality and applicability of the asymmetric photoaerobic selenium-π-acid catalysis in a synthetic context, we implemented the title protocol in a concise enantioselective synthesis of protected *trans*-2,3-*cis*-3,4-dihydroxyproline (**11**) (Scheme 6). 3,4-Dihydroxyprolines are frequently found in living organisms serving as constituents, for instance, in cell walls of diatoms, in fungal toxins, or in adhesive proteins of mussels, and are also associated with

Scheme 6. Seven-Step Enantioselective Synthesis of Protected (2S,3R,4S)-3,4-Dihydroxyproline (11)
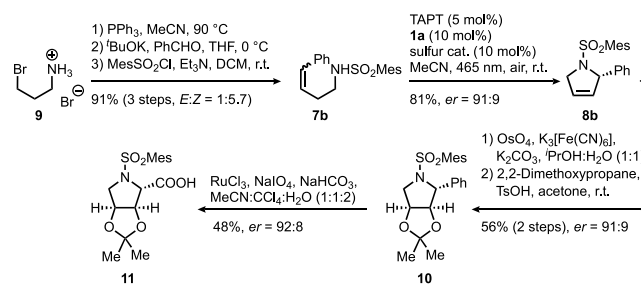
inhibitory activities toward glucosidase enzymes.[51,52] Asymmetric syntheses of 3,4-dihydroxyprolines have been accomplished, inter alia, by Martin et al. in 2002[53] and Davies et al. in 2006[54] in 9 and 12 steps, respectively. We reasoned that 3-pyrrolines **8b** not only provide the full carbon skeleton of the target compound but also offer an expedient functional group pattern to install the requisite periphery around the pyrrolidine core under substrate stereocontrol. We started with the formation of a phosphonium salt derived from commercial 3-bromopropyl hydrobromide (**9**), followed by the Wittig reaction and N-sulfonylation to generate **7b** in a 91% yield as an isomeric mixture (E/Z = 1:5.7, Scheme 6). Upon enantioselective cycloamination (81%, er = 91:9), **8b** was *syn*-dihydroxylated with OsO$_4$ and potassium ferricyanide and subsequently converted into acetonide **10** with an er of 91:9. Oxidative degradation of the phenyl group into a free carboxylic acid afforded target **11** in a total number of 7 steps and an overall yield of 20%, which represents the shortest enantioselective synthesis of this compound class to date.

■ CONCLUSIONS

In summary, we have developed a modular approach toward chiral, nonracemic spirobiindane selenium-π-acid catalysts, which enable for the first time very enantioselective aerobic photoredox-catalytic cyclofunctionalizations of simple, nondirecting alkenes. Through ternary disulfide cocatalysis, a broad series of enoic acids and unsaturated sulfonamides were cyclized into enantiomerically highly enriched butenolides and 3-pyrrolines, respectively, with very good tolerance for both conjugated and nonconjugated alkene substrates as well as excellent 5-*endo*-trig selectivity. Mechanistically, the sulfur cocatalyst is proposed to serve two critical purposes (Schemes S11 and S12):[31] (1) in combination with the photoredox cocatalyst, the disulfide is believed to function as an electron transfer catalyst that interacts with selenenylated intermediates in the catalytic cycle. (2) The disulfide presumably accelerates the final step in the catalytic cycle (i.e., β-elimination),[31,49] which seems rate limiting under the title conditions. Future efforts will be directed toward a generalized applicability of chiral selenium-π-acids in air-driven photoredox-multicatalytic regimes such as enantioselective intermolecular allylic functionalizations and 1,2-difunctionalizations.

■ ASSOCIATED CONTENT

ⓢ Supporting Information

The Supporting Information is available free of charge at https://pubs.acs.org/doi/10.1021/acscatal.3c04443.

Materials and methods; conditions optimization and general experimental procedures; gram-scale reaction;

control experiments; characterization data of all products; and copies of ^{1}H, ^{13}C, ^{19}F, ^{31}P, and ^{77}Se spectra of all products (PDF)

AUTHOR INFORMATION

Corresponding Author

Alexander Breder − Institut Für Organische Chemie, Universität Regensburg, 93053 Regensburg, Germany; orcid.org/0000-0003-4899-5919; Email: alexander.breder@ur.de

Authors

Tao Lei − Institut Für Organische Chemie, Universität Regensburg, 93053 Regensburg, Germany

Sebastian Graf − Institut Für Organische Chemie, Universität Regensburg, 93053 Regensburg, Germany

Christopher Schöll − Institut Für Organische Chemie, Universität Regensburg, 93053 Regensburg, Germany

Felix Krätzschmar − Institut Für Organische Chemie, Universität Regensburg, 93053 Regensburg, Germany

Bernhard Gregori − Institut Für Organische Chemie, Universität Regensburg, 93053 Regensburg, Germany

Theresa Appleson − Institut Für Organische Chemie, Universität Regensburg, 93053 Regensburg, Germany

Complete contact information is available at:
https://pubs.acs.org/10.1021/acscatal.3c04443

Author Contributions

†T.L. and S.G. contributed equally to this study.

Notes

The authors declare no competing financial interest.

REFERENCES

(1) (a) Sharpless, K. B. Searching for New Reactivity (Nobel Lecture) Copyright The Nobel Foundation 2002. We thank the Nobel Foundation, Stockholm, for permission to print this lecture. Adapted with the permission of the editors from "Coelacanths and Catalysis": K. B. Sharpless, Tetrahedron 1994, 50, 4235. Angew. Chem., Int. Ed. 2002, 41, 2024−2032. (b) Noyori, R. Asymmetric Catalysis: Science and Opportunities (Nobel Lecture 2001). Adv. Synth. Catal. 2003, 345, 15−32. (c) Knowles, W. S. Asymmetric Hydrogenations (Nobel Lecture 2001). Adv. Synth. Catal. 2003, 345, 3−13.

(2) (a) Prentice, C.; Morrisson, J.; Smith, A. D.; Zysman-Colman, E. Recent Developments in Enantioselective Photocatalysis. Beilstein J. Org. Chem. 2020, 16, 2363−2441. (b) Genzink, M. J.; Kidd, J. B.; Swords, W. B.; Yoon, T. P. Chiral Photocatalyst Structures in Asymmetric Photochemical Synthesis. Chem. Rev. 2022, 122, 1654−1716. (c) Mondal, S.; Dumur, F.; Gigmes, D.; Sibi, M. P.; Bertrand, M. P.; Nechab, M. Enantioselective Radical Reactions Using Chiral Catalysts. Chem. Rev. 2022, 122, 5842−5976.

(3) (a) Nicewicz, D. A.; MacMillan, D. W. C. Merging Photoredox Catalysis with Organocatalysis: The Direct Asymmetric Alkylation of Aldehydes. Science 2008, 322, 77−80. (b) DiRocco, D. A.; Rovis, T. Catalytic Asymmetric α-Acylation of Tertiary Amines Mediated by a Dual Catalysis Mode: N-Heterocyclic Carbene and Photoredox Catalysis. J. Am. Chem. Soc. 2012, 134, 8094−8097. (c) Zhu, Y.; Zhang, L.; Luo, S. Asymmetric α-Photoalkylation of β-Ketocarbonyls by Primary Amine Catalysis: Facile Access to Acyclic All-Carbon Quaternary Stereocenters. J. Am. Chem. Soc. 2014, 136, 14642−14645. (d) Du, J.; Skubi, K. L.; Schultz, D. M.; Yoon, T. P. A Dual-Catalysis Approach to Enantioselective [2 + 2] Photocycloadditions Using Visible Light. Science 2014, 344, 392−396. (e) Capacci, A. G.; Malinowski, J. T.; McAlpine, N. J.; Kuhne, J.; MacMillan, D. W. C. Direct, enantioselective α-alkylation of aldehydes using simple olefins. Nat. Chem. 2017, 9, 1073−1077. (f) Biegasiewicz, K. F.; Cooper, S. J.; Emmanuel, M. A.; Miller, D. C.; Hyster, T. K. Catalytic Promiscuity Enabled by Photoredox Catalysis in Nicotinamide-dependent Oxidoreductases. Nat. Chem. 2018, 10, 770−775.

(4) (a) Proctor, R. S. J.; Davis, H. J.; Phipps, R. J. Catalytic Enantioselective Minisci-type Addition to Heteroarenes. Science 2018, 360, 419−422. (b) Yin, Y.; Dai, Y.; Jia, H.; Li, J.; Bu, L.; Qiao, B.; Zhao, X.; Jiang, Z. Conjugate Addition−Enantioselective Protonation of N-Aryl Glycines to α-Branched 2-Vinylazaarenes via Cooperative Photoredox and Asymmetric Catalysis. J. Am. Chem. Soc. 2018, 140, 6083−6087. (c) Nakano, Y.; Black, M. J.; Meichan, A. J.; Sandoval, B. A.; Chung, M. M.; Biegasiewicz, K. F.; Zhu, T.; Hyster, T. K. Photoenzymatic Hydrogenation of Heteroaromatic Olefins Using "Ene"-Reductases with Photoredox Catalysts. Angew. Chem., Int. Ed. 2020, 59, 10484−10488.

(5) (a) Lian, M.; Li, Z.; Cai, Y.; Meng, Q.; Gao, Z. Enantioselective photooxygenation of β-keto esters by chiral phase-transfer catalysis using molecular oxygen. Chem.—Asian J. 2012, 7, 2019−2023. (b) Woźniak, Ł.; Murphy, J. J.; Melchiorre, P. Photo-organocatalytic Enantioselective Perfluoroalkylation of β-Ketoesters. J. Am. Chem. Soc. 2015, 137, 5678−5681. (c) Ding, W.; Lu, L.-Q.; Zhou, Q. Q.; Wei, Y.; Chen, J.-R.; Xiao, W.-J. Bifunctional Photocatalysts for Enantioselective Aerobic Oxidation of β-Ketoesters. J. Am. Chem. Soc. 2017, 139, 63−66.

(6) (a) Bauer, A.; Westkämper, F.; Grimme, S.; Bach, T. Catalytic Enantioselective Reactions Driven by Photoinduced Electron Transfer. Nature 2005, 436, 1139−1140. (b) Huo, H.; Harms, K.; Meggers, E. Catalytic, Enantioselective Addition of Alkyl Radicals to Alkenes via Visible-Light-Activated Photoredox Catalysis with a Chiral Rhodium Complex. J. Am. Chem. Soc. 2016, 138, 6936−6939. (c) Biegasiewicz, K. F.; Cooper, S. J.; Gao, X.; Oblinsky, D. G.; Kim, J. H.; Garfinkle, S. E.; Joyce, L. A.; Sandoval, B. A.; Scholes, G. D.; Hyster, T. K. Photoexcitation of Flavoenzymes Enables a Stereoselective Radical Cyclization. Science 2019, 364, 1166−1169.

(7) (a) Li, Y.; Zhou, K.; Wen, Z.; Cao, S.; Shen, X.; Lei, M.; Gong, L. Copper(II)-Catalyzed Asymmetric Photoredox Reactions: Enantioselective Alkylation of Imines Driven by Visible Light. J. Am. Chem. Soc. 2018, 140, 15850−15858. (b) Guo, X.; Okamoto, Y.; Schreier, M. R.; Ward, T. R.; Wenger, O. S. Enantioselective Synthesis of Amines by Combining Photoredox and Enzymatic Catalysis in a Cyclic Reaction Network. Chem. Sci. 2018, 9, 5052−5056.

(8) (a) Emmanuel, M. A.; Greenberg, N. R.; Oblinsky, D. G.; Hyster, T. K. Accessing Non-natural Reactivity by Irradiating Nicotinamide-dependent Enzymes with Light. Nature 2016, 540, 414−417. (b) Litman, Z. C.; Wang, Y.; Zhao, H.; Hartwig, J. F. Cooperative Asymmetric Reactions Combining Photocatalysis and Enzymatic Catalysis. Nature 2018, 560, 355−359.

(9) (a) Silvi, M.; Verrier, C.; Rey, Y.; Buzzetti, L.; Melchiorre, P. Visible-light Excitation of Iminium Ions Enables the Enantioselective Catalytic β-Alkylation of Enals. Nat. Chem. 2017, 9, 868−873. (b) Woźniak, Ł.; Magagnano, G.; Melchiorre, P. Enantioselective Photochemical Organocascade Catalysis. Angew. Chem., Int. Ed. 2018, 57, 1068−1072. (c) Bonilla, P.; Rey, Y. P.; Holden, C. M.; Melchiorre, P. Photo-Organocatalytic Enantioselective Radical Cascade Reactions of Unactivated Olefins. Angew. Chem., Int. Ed. 2018, 57, 12819−12823. (d) Cao, Z.-Y.; Ghosh, T.; Melchiorre, P. Enantioselective Radical Conjugate Additions Driven by a Photoactive Intramolecular Iminium-ion-based EDA Complex. Nat. Commun. 2018, 9, 3274.

(10) Tutkowski, B.; Meggers, E.; Wiest, O. Understanding Rate Acceleration and Stereoinduction of an Asymmetric Giese Reaction Mediated by a Chiral Rhodium Catalyst. *J. Am. Chem. Soc.* **2017**, *139*, 8062−8065.

(11) (a) Lee, S. H.; Choi, D. S.; Pesic, M.; Lee, Y. W.; Paul, C. E.; Hollmann, F.; Park, C. B. Cofactor-Free, Direct Photoactivation of Enoate Reductases for the Asymmetric Reduction of C = C Bonds. *Angew. Chem., Int. Ed.* **2017**, *56*, 8681−8685. (b) Ye, Y.; Cao, J.; Oblinsky, D. G.; Verma, D.; Prier, C. K.; Scholes, G. D.; Hyster, T. K. Using Enzymes to Tame Nitrogen-centred Radicals for Enantioselective Hydroamination. *Nat. Chem.* **2023**, *15*, 206−212.

(12) Uraguchi, D.; Kimura, Y.; Ueoka, F.; Ooi, T. Urea as a Redox-Active Directing Group under Asymmetric Photocatalysis of Iridium-Chiral Borate Ion Pairs. *J. Am. Chem. Soc.* **2020**, *142*, 19462−19467.

(13) Morse, P. D.; Nguyen, T. M.; Cruz, C. L.; Nicewicz, D. A. Enantioselective Counter-anions in Photoredox Catalysis: The Asymmetric Cation Radical Diels-Alder Reaction. *Tetrahedron* **2018**, *74*, 3266−3272.

(14) For an example of an acridinium-catalyzed asymmetric hydroetherification of unsaturated alcohols governed by a chiral, hydrogen bonding phosphate counterion, see: Yang, Z.; Li, H.; Li, S.; Zhang, M.-T.; Luo, S. A Chiral Ion-pair Photoredox Organocatalyst: Enantioselective Anti-Markovnikov Hydroetherification of Alkenols. *Org. Chem. Front.* **2017**, *4*, 1037−1041.

(15) (a) Guo, Q.; Wang, M.; Peng, Q.; Huo, Y.; Liu, Q.; Wang, R.; Xu, Z. Dual-Functional Chiral Cu-Catalyst-Induced Photoredox Asymmetric Cyanofluoroalkylation of Alkenes. *ACS Catal.* **2019**, *9*, 4470−4476. (b) Zhang, Y.; Sun, Y.; Chen, B.; Xu, M.; Li, C.; Zhang, D.; Zhang, G. Copper-Catalyzed Photoinduced Enantioselective Dual Carbofunctionalization of Alkenes. *Org. Lett.* **2020**, *22*, 1490−1494. (c) Chen, J.; Liang, Y.-J.; Wang, P.-Z.; Li, G.-Q.; Zhang, B.; Qian, H.; Huan, X.-D.; Guan, W.; Xiao, W.-J.; Chen, J.-R. Photoinduced Copper-Catalyzed Asymmetric C-O Cross-Coupling. *J. Am. Chem. Soc.* **2021**, *143*, 13382−13392. (d) Engl, S.; Reiser, O. Copper-photocatalyzed ATRA reactions: concepts, applications, and opportunities. *Chem. Soc. Rev.* **2022**, *51*, 5287−5299. (e) Das, S.; Zhu, C.; Demirbas, D.; Bill, E.; De, C. K.; List, B. Asymmetric Counteranion-directed Photoredox Catalysis. *Science* **2023**, *379*, 494−499.

(16) (a) Ortgies, S.; Depken, C.; Breder, A. Oxidative Allylic Esterification of Alkenes by Cooperative Selenium-Catalysis Using Air as the Sole Oxidant. *Org. Lett.* **2016**, *18*, 2856−2859. (b) Ortgies, S.; Breder, A. Oxidative Alkene Functionalizations via Selenium-π-Acid Catalysis. *ACS Catal.* **2017**, *7*, 5828−5840. (c) Ortgies, S.; Rieger, R.; Rode, K.; Koszinowski, K.; Kind, J.; Thiele, C. M.; Rehbein, J.; Breder, A. Mechanistic and Synthetic Investigations on the Dual Selenium-π-Acid/Photoredox Catalysis in the Context of the Aerobic Dehydrogenative Lactonization of Alkenoic Acids. *ACS Catal.* **2017**, *7*, 7578−7586. (d) Depken, C.; Krätzschmar, F.; Rieger, R.; Rode, K.; Breder, A. Photocatalytic Aerobic Phosphatation of Alkenes. *Angew. Chem., Int. Ed.* **2018**, *57*, 2459−2463. (e) Breder, A.; Rode, K.; Palomba, M.; Ortgies, S.; Rieger, R. Aerobic Allylation of Alcohols with Non-Activated Alkenes Enabled by Light-Driven Selenium-π-Acid Catalysis. *Synthesis* **2018**, *50*, 3875−3885.

(17) (a) Tunge, J. A.; Mellegaard, S. R. Selective Selenocatalytic Allylic Chlorination. *Org. Lett.* **2004**, *6*, 1205−1207. (b) Soloshonok, V. A.; Nelson, D. J. Alkene selenenylation: a Comprehensive Analysis of Relative Reactivities, Stereochemistry and Asymmetric Induction, and Their Comparisons with Sulfenylation. *Beilstein J. Org. Chem.* **2011**, *7*, 744−758. (c) Deng, Z.; Wei, J.; Liao, L.; Huang, H.; Zhao, X. Organoselenium-Catalyzed, Hydroxy-Controlled Regio- and Stereoselective Amination of Terminal Alkenes: Efficient Synthesis of 3-Amino Allylic Alcohols. *Org. Lett.* **2015**, *17*, 1834−1837. (d) Otsuka, Y.; Shimazaki, Y.; Nagaoka, H.; Maruoka, K.; Hashimoto, T. Scalable Synthesis of a Chiral Selenium π-Acid Catalyst and Its Use in Enantioselective Iminolactonization of *β,γ*-Unsaturated Amides. *Synlett* **2019**, *30*, 1679−1682. (e) Singh, F. V.; Wirth, T. Selenium Reagents as Catalysts. *Catal. Sci. Technol.* **2019**, *9*, 1073−1091. (f) Mumford, E. M.; Hemric, B. N.; Denmark, S. E. Catalytic, Enantioselective Syn-Oxyamination of Alkenes. *J. Am. Chem. Soc.*

2021, *143*, 13408−13417. (g) Yang, L.; Liu, Y.; Fan, W. X.; Tan, D. H.; Li, Q.; Wang, H. Regiocontrolled Allylic Functionalization of Internal Alkene via Selenium-π-acid Catalysis Guided by Boron Substitution. *Chem. Sci.* **2022**, *13*, 6413−6417.

(18) (a) Lampard, C.; Murphy, J. A.; Lewis, N. Tetrathiafulvalene as a Catalyst for Radical-polar Crossover Reactions. *J. Chem. Soc., Chem. Commun.* **1993**, 295−297. (b) Murphy, J. A.; Rasheed, F.; Roome, S. J.; Lewis, N. Termination of Radical-polar Crossover Reactions by Intramolecular Nucleophiles. *Chem. Commun.* **1996**, 737−738. (c) Yi, H.; Niu, L.; Song, C.; Li, Y.; Dou, B.; Singh, A. K.; Lei, A. Photocatalytic Dehydrogenative Cross-Coupling of Alkenes with Alcohols or Azoles without External Oxidant. *Angew. Chem., Int. Ed.* **2017**, *56*, 1120−1124. (d) Reed, N. L.; Lutovsky, G. A.; Yoon, T. P. Copper-Mediated Radical-Polar Crossover Enables Photocatalytic Oxidative Functionalization of Sterically Bulky Alkenes. *J. Am. Chem. Soc.* **2021**, *143*, 6065−6070. (e) Sharma, S.; Singh, J.; Sharma, A. Visible Light Assisted Radical-Polar/Polar-Radical Crossover Reactions in Organic Synthesis. *Adv. Synth. Catal.* **2021**, *363*, 3146−3169.

(19) Reed, N. L.; Yoon, T. P. Oxidase Reactions in Photoredox Catalysis. *Chem. Soc. Rev.* **2021**, *50*, 2954−2967.

(20) (a) Krätzschmar, F.; Ortgies, S.; Willing, R. Y. N.; Breder, A. Rational Design of Chiral Selenium-π-Acid Catalysts. *Catalysts* **2019**, *9*, 153. (b) For a related study on enantioselective oxicyclizations, see: Qi, Z.-C.; Li, Y.; Wang, J.; Ma, L.; Wang, G.-W.; Yang, S.-D. Electrophilic Selenium-Catalyzed Desymmetrizing Cyclization to Access *P*-Stereogenic Heterocycles. *ACS Catal.* **2023**, *13*, 13301−13309.

(21) For a related study on asymmetric cyclofunctionalizations (ee's ranged from 3 to 7%) of enoic acids via H-bond-photoredox-multicatalysis, see: Álvaro, M.; Formentín, P.; García, H.; Palomares, E.; Sabater, M. J. Chiral *N*-Alkyl-2,4,6-triphenylpyridiniums as Enantioselective Triplet Photosensitizers. Laser Flash Photolysis and Preparative Studies. *J. Org. Chem.* **2002**, *67*, 5184−5189.

(22) (a) Kalyani, D.; Kornfilt, D. J.-P.; Burk, M. T.; Denmark, S. E. In *Lewis Base Catalysis in Organic Synthesis*; Eds: Vedejs, E., Denmark, S. E., Eds.; Wiley VCH: Weinheim, Germany, 2016; Vol. 3, chapter 24. (b) Kawamata, Y.; Hashimoto, T.; Maruoka, K. A Chiral Electrophilic Selenium Catalyst for Highly Enantioselective Oxidative Cyclization. *J. Am. Chem. Soc.* **2016**, *138* (16), 5206−5209. (c) Tao, Z.; Gilbert, B. B.; Denmark, S. E. Catalytic, Enantioselective syn-Diamination of Alkenes. *J. Am. Chem. Soc.* **2019**, *141*, 19161−19170.

(23) (a) Brewster, J. H.; Prudence, R. T. Useful Model of Optical Activity. X. Absolute Configuration and Chiroptical Properties of Optically Active 1,1′-Spirobiindan, 1,1′-Spirobiindene, and 1,1′-Spirobiindanone. *J. Am. Chem. Soc.* **1973**, *95*, 1217−1229. (b) Hill, R. K.; Cullison, D. A. Dissymmetric spirans. II. Absolute configuration of 1,1′-spirobiindene and related compounds. *J. Am. Chem. Soc.* **1973**, *95*, 1229−1239. (c) Birman, V. B.; L Rheingold, A.; Lam, K.-C. 1,1′-Spirobiindane-7,7′-diol: a novel, C_2-symmetric chiral ligand. *Tetrahedron: Asymmetry* **1999**, *10*, 125−131. (d) Zhang, J.-H.; Liao, J.; Cui, X.; Yu, K.-B.; Zhu, J.; Deng, J.-G.; Zhu, S.-F.; Wang, L.-X.; Zhou, Q.-L.; Chung, L. W.; Ye, T. Highly efficient and practical resolution of 1,1′-spirobiindane-7,7′-diol by inclusion crystallization with *N*-benzylcinchonidinium chloride. *Tetrahedron: Asymmetry* **2002**, *13*, 1363−1366. (e) Fu, Y.; Xie, J.-H.; Hu, A.-G.; Zhou, H.; Wang, L.-X.; Zhou, Q.-L. Novel monodentate spiro phosphorus ligands for rhodium-catalyzed hydrogenation reactions. *Chem. Commun.* **2002**, 480−481. (f) Xie, J.-H.; Zhou, Q.-L. Chiral Diphosphine and Monodentate Phosphorus Ligands on a Spiro Scaffold for Transition-Metal-Catalyzed Asymmetric Reactions. *Acc. Chem. Res.* **2008**, *41*, 581−593. (g) Chung, Y. K.; Fu, G. C. Phosphine-Catalyzed Enantioselective Synthesis of Oxygen Heterocycles. *Angew. Chem., Int. Ed.* **2009**, *48*, 2225−2227. (h) Ćorić, I.; Müller, S.; List, B. Kinetic Resolution of Homoaldols via Catalytic Asymmetric Transacetalization. *J. Am. Chem. Soc.* **2010**, *132*, 17370−17373. (i) Zhu, S.-F.; Zhou, Q.-L. Transition-Metal-Catalyzed Enantioselective Heteroatom-Hydrogen Bond Insertion Reactions. *Acc. Chem. Res.* **2012**, *45*, 1365−1377. (j) Zheng, J.; Cui, W.-J.; Zheng, C.; You, S.-L. Synthesis and Application of Chiral Spiro Cp Ligands in Rhodium-Catalyzed

Asymmetric Oxidative Coupling of Biaryl Compounds with Alkenes. *J. Am. Chem. Soc.* **2016**, *138*, 5242−5245.

(24) (a) Sun, W.; Gu, H.; Lin, X. Synthesis and Application of Hexamethyl-1,1'-spirobiindane-Based Phosphine-Oxazoline Ligands in Ni-Catalyzed Asymmetric Arylation of Cyclic Aldimines. *J. Org. Chem.* **2018**, *83*, 4034−4043. (b) Lin, X.; Zhou, Q.; Pan, R.; Shan, H. Synthesis and Optical Resolution of 3,3,3',3'-Tetramethyl-1,1-spirobiindane-7,7'-diol. *Synthesis* **2019**, *51*, 557−563.

(25) (a) Gu, H.; Han, Z.; Xie, H.; Lin, X. Iron-Catalyzed Enantioselective Si-H Bond Insertions. *Org. Lett.* **2018**, *20*, 6544−6549. (b) Shan, H.; Zhou, Q.; Yu, J.; Zhang, S.; Hong, X.; Lin, X. Rhodium-Catalyzed Asymmetric Addition of Organoboronic Acids to Aldimines Using Chiral Spiro Monophosphite-Olefin Ligands: Method Development and Mechanistic Studies. *J. Org. Chem.* **2018**, *83*, 11873−11885.

(26) Manna, T.; Misra, A. K. On-water Synthesis of Glycosyl Selenocyanate Derivatives and Their Application in the Metal Free Organocatalytic Preparation of Nonglycosidic Selenium Linked Pseudodisaccharide Derivatives. *RSC Adv.* **2021**, *11*, 10902−10911.

(27) Shan, H.; Pan, R.; Lin, X. Synthesis and Application of A New Chiral Monodentate Spiro Phosphoramidite Ligand Based on Hexamethyl-1,1'-spirobiindane Backbone in Asymmetric Hydroamination/arylation of Alkenes. *Org. Biomol. Chem.* **2018**, *16*, 6183−6186.

(28) Molteni, V.; Rhodes, D.; Rubins, K.; Hansen, M.; Bushman, F. D.; Siegel, J. S. A New Class of HIV-1 Integrase Inhibitors: The 3,3,3',3'-Tetramethyl-1,1'-spirobi(indan)-5,5',6,6'-tetrol Family. *J. Med. Chem.* **2000**, *43*, 2031−2039.

(29) Zheng, Z.; Cao, Y.; Chong, Q.; Han, Z.; Ding, J.; Luo, C.; Wang, Z.; Zhu, D.; Zhou, Q.-L.; Ding, K. Chiral Cyclohexyl-Fused Spirobiindanes: Practical Synthesis, Ligand Development, and Asymmetric Catalysis. *J. Am. Chem. Soc.* **2018**, *140*, 10374−10381.

(30) For further optimizations with other photocatalysts, see Schemes S1, S3 in the Supporting Information. For a detailed screening of additives not mentioned in Scheme 3, see Supporting Information, Scheme S2.

(31) Additional detailed mechanistic investigation on the rate accelerating effect of sulfur cocatalysts in selenium-π-acid catalyzed reactions are ongoing in our laboratories and will be reported elsewhere.

(32) Gusev, D. G.; Ozerov, O. V. Calculated Hydride and Fluoride Affinities of a Series of Carbenium andSilylium Cations in the Gas Phase and in C_6H_5Cl Solution. *Chem.—Eur. J.* **2011**, *17*, 634−640.

(33) (a) Wirth, T. Asymmetric Reaction of Arylalkenes with Diselenides. *Angew. Chem., Int. Ed.* **1995**, *34*, 1726−1728. (b) Fujita, K.; Murata, K.; Iwaoka, M.; Tomoda, S. Design of optically active selenium reagents having a chiral tertiary amino group and their application to asymmetric inter- and intramolecular oxyselenenylations. *Tetrahedron* **1997**, *53*, 2029−2048.

(34) (a) Zheng, Z.; Cao, Y.; Zhu, D.; Wang, Z.; Ding, K. Development of Chiral Spiro Phosphoramidites for Rhodium-Catalyzed Enantioselective Reactions. *Chem.—Eur. J.* **2019**, *25*, 9491−9497.

(35) (a) Hevesi, L.; Krief, A. Photo-Oxygenation of Selenides: A New Pathway to Selenoxides. *Angew. Chem., Int. Ed.* **1976**, *15*, 381. (b) Krief, A.; Lonez, F. Singlet Oxygen Oxidation of Selenides to Selenoxides. *Tetrahedron Lett.* **2002**, *43*, 6255−6257.

(36) Gevorgyan, A.; Mkrtchyan, S.; Grigoryan, T.; Iaroshenko, V. O. Disilanes as Oxygen Scavengers and Surrogates of Hydrosilanes Suitable for Selective Reduction of Nitroarenes, Phosphine Oxides and Other Valuable Substrates. *Org. Chem. Front.* **2017**, *4*, 2437−2444.

(37) Constable, D. J. C.; Curzons, A. D.; Cunningham, V. L. Metrics to "Green" Chemistry: Which Are the Best? *Green Chem.* **2002**, *4*, 521−527.

(38) (a) Browne, D. M.; Niyomura, O.; Wirth, T. Catalytic Use of Selenium Electrophiles in Cyclizations. *Org. Lett.* **2007**, *9*, 3169−3171.

(39) An exception to this trend of lowered yields with sterically demanding substituents was found in butenolide **6q**. The reasons for this anomalous outcome are not fully clear at this point.

(40) (a) Rondeau, D.; Gill, P.; Chan, M.; Curry, K.; Lubell, W. D. Synthesis and Pharmacology of New Enantiopure Δ3−4-Arylkainoids. *Bioorg. Med. Chem. Lett.* **2000**, *10*, 771−773. (b) Mou, Q.-Y.; Chen, J.; Zhu, Y.-C.; Zhou, D.-H.; Chi, Z.-Q.; Long, Y.-Q. 3-Pyrroline Containing Arylacetamides: A Novel Series of Remarkably Selective κ-Agonists. *Bioorg. Med. Chem. Lett.* **2002**, *12*, 2287−2290. (c) Magedov, I. V.; Luchetti, G.; Evdokimov, N. M.; Manpadi, M.; Steelant, W. F. A.; Van slambrouck, S.; Tongwa, P.; Antipin, M. Y.; Kornienko, A. Novel Three-component Synthesis and Antiproliferative Properties of Diversely Functionalized Pyrrolines. *Bioorg. Med. Chem. Lett.* **2008**, *18*, 1392−1396. (d) Medran, N. S.; La-Venia, A.; Testero, S. A. Metal-mediated Synthesis of Pyrrolines. *RSC Adv.* **2019**, *9*, 6804−6844. (e) Kerru, N.; Gummidi, L.; Maddila, S.; Gangu, K. K.; Jonnalagadda, S. B. A Review on Recent Advances in Nitrogen-Containing Molecules and Their Biological Applications. *Molecules* **2020**, *25*, 1909.

(41) (a) Jones, A. D.; Knight, D. W.; Redfern, A. L.; Gilmore, J. Selenocyclisations of Homoallylic Sulfonamides: A Highly Stereoselective Route to Both cis- and trans-2,5-Dihydropyrroles. *Tetrahedron Lett.* **1999**, *40*, 3267−3270. (b) Viso, A.; Fernández de la Pradilla, R.; Ureña, M.; Colomer, I. Highly Diastereoselective Addition of Lithio Vinyl Sulfoxides to N-Sulfinimines: An Entry to Enantiopure 3-Sulfinyl-2,5-cis-dihydropyrroles. *Org. Lett.* **2008**, *10*, 4775−4778. (c) Pandey, G.; Laha, R.; Mondal, P. K. Heterocyclization Involving Benzylic C(sp^3)-H Functionalization Enabled by Visible Light Photoredox Catalysis. *Chem. Commun.* **2019**, *55*, 9689−9692.

(42) (a) Kagoshima, H.; Okamura, T.; Akiyama, T. The Asymmetric [3 + 2] Cycloaddition Reaction of Chiral Alkenyl Fischer Carbene Complexes with Imines: Synthesis of Optically Pure 2,5-Disubstituted-3-pyrrolidinones. *J. Am. Chem. Soc.* **2001**, *123*, 7182−7183. (b) Fang, Y.-Q.; Jacobsen, E. N. Cooperative, Highly Enantioselective Phosphinothiourea Catalysis of Imine-Allene [3 + 2] Cycloadditions. *J. Am. Chem. Soc.* **2008**, *130*, 5660−5661. (c) Han, X.; Zhong, F.; Wang, Y.; Lu, Y. Versatile Enantioselective [3 + 2] Cyclization between Imines and Allenoates Catalyzed by Dipeptide-Based Phosphines. *Angew. Chem., Int. Ed.* **2012**, *51*, 767−770. (d) Henry, C. E.; Xu, Q.; Fan, Y. C.; Martin, T. J.; Belding, L.; Dudding, T.; Kwon, O. Hydroxyproline-Derived Pseudoenantiomeric [2.2.1] Bicyclic Phosphines: Asymmetric Synthesis of (+)- and (−)-Pyrrolines. *J. Am. Chem. Soc.* **2014**, *136*, 11890−11893. (e) Kramer, S.; Fu, G. C. Use of a New Spirophosphine To Achieve Catalytic Enantioselective [4 + 1] Annulations of Amines with Allenes To Generate Dihydropyrroles. *J. Am. Chem. Soc.* **2015**, *137*, 3803−3806.

(43) (a) Winter, C.; Krause, N. Structural Diversity through Gold Catalysis: Stereoselective Synthesis of N-Hydroxypyrrolines, Dihydroisoxazoles, and Dihydro-1,2-oxazines. *Angew. Chem., Int. Ed.* **2009**, *48*, 6339−6342. (b) Cheng, X.; Zhang, L. Chiral Bifunctional Phosphine Ligand Enables Gold-Catalyzed Asymmetric Isomerization and Cyclization of Propargyl Sulfonamide into Chiral 3-Pyrroline. *Org. Lett.* **2021**, *23*, 8194−8198.

(44) (a) Dieter, R. K.; Chen, N.; Gore, V. K. Reaction of α-(N-Carbamoyl)alkylcuprates with Enantioenriched Propargyl Electrophiles: Synthesis of Enantioenriched 3-Pyrrolines. *J. Org. Chem.* **2006**, *71*, 8755−8760. (b) Wu, W.-Q.; Peng, Q.; Dong, D.-X.; Hou, X.-L.; Wu, Y.-D. A Dramatic Switch of Enantioselectivity in Asymmetric Heck Reaction by Benzylic Substituents of Ligands. *J. Am. Chem. Soc.* **2008**, *130*, 9717−9725. (c) Yang, Z.; Zhou, J. Palladium-Catalyzed, Asymmetric Mizoroki-Heck Reaction of Benzylic Electrophiles Using Phosphoramidites as Chiral Ligands. *J. Am. Chem. Soc.* **2012**, *134*, 11833−11835.

(45) (a) Hartung, J.; Dornan, P. K.; Grubbs, R. H. Enantioselective Olefin Metathesis with Cyclometalated Ruthenium Complexes. *J. Am. Chem. Soc.* **2014**, *136*, 13029−13037. (b) Groso, E. J.; Golonka, A. N.; Harding, R. A.; Alexander, B. W.; Sodano, T. M.; Schindler, C. S.

3-Aryl-2,5-Dihydropyrroles via Catalytic Carbonyl-Olefin Metathesis. *ACS Catal.* **2018**, *8*, 2006−2011.

(46) For a sequential asymmetric synthesis of a 3-pyrroline derivative via catalytic enantioselective 1,2-bromocycloamination and base-promoted dehydrodebromination, see: Chen, J.; Zhou, L.; Yeung, Y.-Y. A highly enantioselective approach towards 2-substituted 3-bromopyrrolidines. *Org. Biomol. Chem.* **2012**, *10*, 3808−3811.

(47) Burns, N. Z.; Baran, P. S.; Hoffmann, R. W. Redox Economy in Organic Synthesis. *Angew. Chem., Int. Ed.* **2009**, *48*, 2854−2867.

(48) Guo, R.; Huang, J.; Huang, H.; Zhao, X. Organoselenium-Catalyzed Synthesis of Oxygen- and Nitrogen-Containing Heterocycles. *Org. Lett.* **2016**, *18*, 504−507.

(49) Wilken, M.; Ortgies, S.; Breder, A.; Siewert, I. Mechanistic Studies on the Anodic Functionalization of Alkenes Catalyzed by Diselenides. *ACS Catal.* **2018**, *8*, 10901−10912.

(50) The absolute configuration of **8a** was determined by comparison with its reported enantiomer. It is assumed that catalyst **1a** sets the same absolute configuration in all other products **8**. Feng, B.; Cheng, H.-G.; Chen, J.-R.; Deng, Q.-H.; Lu, L.-Q.; Xiao, W.-J. Palladium/sulfoxide−phosphine-catalyzed highly enantioselective allylic etherification and amination. *Chem. Commun.* **2014**, *50*, 9550−9553.

(51) (a) Weir, C. A.; Taylor, C. M. Synthesis of a Protected 3,4-Dihydroxyproline from a Pentose Sugar. *Org. Lett.* **1999**, *1*, 787−789. (b) Nakajima, T.; Volcani, B. E. 3,4-Dihydroxyproline: A New Amino Acid in Diatom Cell Walls. *Science* **1969**, *164*, 1400−1401. (c) Buku, A.; Faulstich, H.; Wieland, T.; Dabrowski, J. 2,3-trans-3,4-trans-3,4-Dihydroxy-L-proline: An Amino Acid in Toxic Peptides of Amanita Virosa Mushrooms. *Proc. Natl. Acad. Sci. U.S.A.* **1980**, *77*, 2370−2371. (d) Taylor, S. W.; Waite, J. H.; Ross, M. M.; Shabanowitz, J.; Hunt, D. F. Trans-2,3-cis-3,4-Dihydroxyproline, a New Naturally Occurring Amino Acid, Is the Sixth Residue in the Tandemly Repeated Consensus Decapeptides of an Adhesive Protein from Mytilus edulis. *J. Am. Chem. Soc.* **1994**, *116*, 10803−10804.

(52) (a) Ganem, B. Inhibitors of Carbohydrate-Processing Enzymes: Design and Synthesis of Sugar-Shaped Heterocycles. *Acc. Chem. Res.* **1996**, *29*, 340−347. (b) Sears, P.; Wong, C. H. Mechanism-based Inhibition of Carbohydrate-mediated Biological Recognitions. *Chem. Commun.* **1998**, 1161−1170. (c) Sinnott, M. L. Catalytic Mechanism of Enzymic Glycosyl Transfer. *Chem. Rev.* **1990**, *90*, 1171−1202.

(53) Martín, R.; Alcón, M.; Pericàs, M. A.; Riera, A. Ring-Closing Metathesis of Chiral Allylamines. Enantioselective Synthesis of (2S,3R,4S)-3,4-Dihydroxyproline. *J. Org. Chem.* **2002**, *67*, 6896−6901.

(54) Davis, F. A.; Ramachandar, T.; Chai, J.; Skucas, E. Asymmetric Synthesis of α-Amino Aldehydes from Sulfinimine (N-sulfinyl imine)-derived α-amino 1,3-dithianes. Formal Synthesis of (−)-2,3-trans-3,4-cis-dihydroxyproline. *Tetrahedron Lett.* **2006**, *47*, 2743−2746.